Common OECD/NEA FIRE and PRISME Cable Benchmark Exercise

W Plumecocq, S Bascou, M Röewekamp, K Hamburger

Common OECD/NEA FIRE and PRISME Cable Benchmark Exercise

W. Plumecocq[a*], S. Bascou[a], M. Röewekamp[b], K. Hamburger[c]

[a]Institut de Radioprotection et de Sûreté Nucléaire (IRSN), Cadarache, France,
[b]Gesellschaft für Anlagen- und Reaktorsicherheit (GRS) gGmbH, Köln, Germany
[c]Nuclear Regulatory Commission (NRC), Maryland, United States of America
* Corresponding author. Tel.: +33 442 199 657; Fax: +33 442 199 1653
E-mail address: william.plumecocq@irsn.fr

Abstract

This paper deals with the common OECD/NEA FIRE and PRISME Cable Benchmark Exercise conducted for a realistic cable fire scenario in an electrical system of a nuclear power plant. The major goal was to simulate a real cable fire event in order to assess the behaviour of fire models for a complex and real fire scenario with the current state of knowledge. Since a numerical Benchmark Exercise on a real fire event is quite challenging, a three-step methodology was adopted: (1) a calibration phase of the cable fire models, (2) a blind simulation of a cable fire test, and (3) the real cable fire event simulation. The selected fire event from the FIRE Database occurred in 2014 in a heater bay of a nuclear power plant. Thirteen institutions from nine NEA member countries participated in this Benchmark Exercise. Simulations were performed using computational fluid dynamics codes, a lumped parameter code, and zone codes. The simulations have provided a wide range of results which reflect the difficulty for fire simulation codes to correctly predict the development of the fire heat release rate over time of a cable tray fire, even under simple, open atmosphere conditions.

Keyword: Benchmark Exercise, Cable fire, Real fire event, Cable fire simulations

1. Introduction

Based on a request in 2016 from the Fire Incidents Records Exchange (FIRE) Database project of the Nuclear Energy Agency (NEA) of the Organization for Economic Co-operation and Development (OECD), the PRISME 2 Program Review Group (PRG) made the recommendation that there should be a common Benchmark Exercise on a realistic cable fire that resembles, as closely as possible, a real cable fire event included in the FIRE Database, using information on electrical cable fires from the OECD/NEA PRISME projects. This led to the joint venture of the two OECD/NEA projects called “Common OECD/NEA FIRE and PRISME Cable Benchmark Exercise”.

Observations from the FIRE Database [1],[2] have clearly demonstrated the significance of fire events involving cables and shown that a majority of these events were either safety-related or had the potential to impair nuclear safety. On this topic, PRISME 2 cable fire experiments [3],[4] have significantly increased the knowledge regarding cable fire behaviour and investigated various types of cables implemented in nuclear power plants (NPPs) in member states.

The major goal of this Benchmark Exercise is to simulate a real cable fire event in order to assess the behaviour of fire models for such a complex and real fire scenario with the current state of knowledge. The strong interest of experts from regulators, technical safety

organizations (TSOs) and licensees in predicting cable fires shows that such a Benchmark Exercise is a unique opportunity for cross-cutting work between experts from the OECD/NEA FIRE and PRISME Projects. Due to significant interest, a decision was made to open the Common OECD/NEA FIRE and PRISME Cable Benchmark Exercise to other CSNI (Committee on the Safety of Nuclear Installations) member countries.

The latest version of the OECD/NEA FIRE Database (2017:02) [5] was released in May 2019, gathering more than 500 fire events recorded up to the end of 2017. The criteria for the cable tray fire event selection, as prescribed by the PRISME 2 PRG members, are the following:

- a cable fire scenario with flames and smoke
- a quite recent event (from about the last ten years)
- a sufficiently well-documented event
- the significance of being able to receive additional information
- the closeness to PRISME cable fire experimental scenarios
- preferably only one compartment involved in the fire
- a fire duration between 15 min and 60 min

A shortlist of four potential candidates providing a quite detailed description of the ignition phase and the sequences of the events from the available information was established. The ability to gather enough data on the event from licensees supporting the activity was the decisive criterion for the final event selection. Based on all the prerequisites, the real fire event that was finally selected occurred in 2014 in a heater bay of a NPP and involved two horizontal electrical cable trays, mainly loaded with Polyvinyl Chloride (PVC) insulated cables.

2. The heater bay fire event

The authors emphasize that specific details on the fire event, in particular information on the identified NPP where the fire occurred, remain undisclosed due to confidentiality matters.

The selected fire event occurred in the heater bay of the turbine building of a NPP. The fire involved two 0.90 m wide horizontal cable trays mainly loaded with PVC insulated cables and was caused by a non-conforming cable routing. The fire started by the self-ignition of 120 V power cables due to an arc fault. It was initiated when the high humidity and condensate from a steam leak (see Fig. 1) provided the environment necessary for the existing flaw in an electrical cable to short to ground.

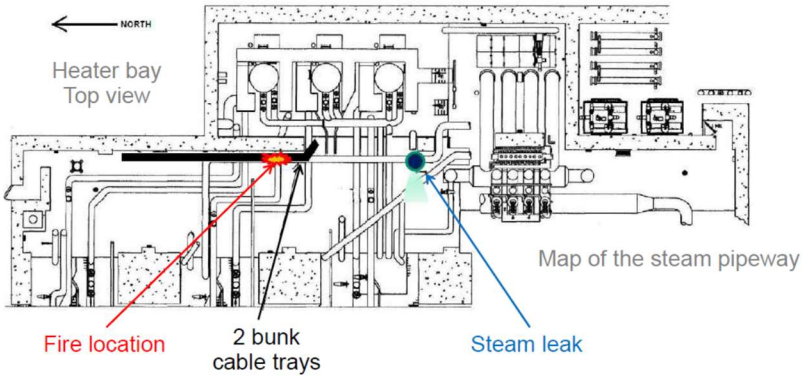

Fig 1. Top view scheme of the heater bay.

The source of the cable flaw was identified as cable routing inconsistent with the current standard for minimum static bend radius for this type and size of cable, i.e., resting across rungs on a horizontal cable tray and exiting at a sharp angle downward into a 12 m vertical run, as illustrated in Fig 2.

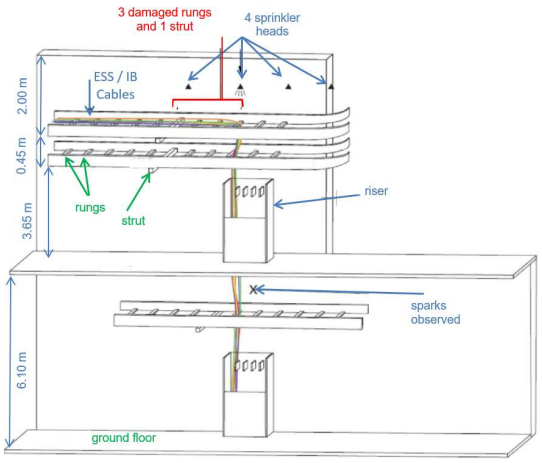

Fig. 2. Front view scheme of the cable routine in the heater bay.

The fire duration between ignition and successful extinction by wet pipe sprinkler was estimated to be approximately 20 min (± 2 min). Investigations by the licensee provided a detailed description of the fire behaviour and the sequence of the event detailed hereafter.

The non-conforming cable routing concerned three instrument bus (IB) cables and three essential service system (ESS) bus cables. The arc fault from one of the six cables to the rung at the exit point damaged the insulation of nearby cables and heated the rung, leading to the severing of five (2 IB and 3 ESS) of the six cables. This conclusion is based on in-situ examination recording the remaining riser portion of each of the five cables, of equal length, with severed ends at the rung, and the remaining horizontal portions of two of the ESS bus cables also aligned with the rung. When they were severed, the two-line cables for the IB feed arc faulted together. These cables continued to arc until approximately 0.61 m of copper had been melted from each of the IB line cables.

The arc fault between the IB line cables ended at a strut support, as evidenced by the ends of the IB cables being found aligning with and in the molten portion of the strut. It is likely that the breaker for the IB feed tripped at this time, as evidenced by the remaining intact copper. The total time from the initial arc fault to the IB feed breaker trip is estimated to be approximately 1 min, corresponding to the time when sparks were observed outside the heater bay, and the time of the swap of the IB from its main feed to a backup feed.

The fire on the lower tray was initiated by debris falling from the fire on the upper tray and radiative heat from the fire source of the upper tray. This is evidenced by the concentration of the damaged cable in the upper levels of the lower tray, with the lower levels undamaged or much less damaged. Additionally, there is no example of molten copper conductor in the lower tray. The fire in the lower tray appears to have continued to burn until extinguished by the fixed fire extinguishing system (wet sprinklers).

Four sprinkler heads were located in the vicinity of the fire, at about 1.20 m to 1.50 m above the top of the upper tray. The sprinkler heads initiate by thermal (fusible) links set to break at 100 °C with a standard response time index (RTI) of about 100 to 360 $m^{0.5}s^{0.5}$ [6]. The heat generated by the fire caused flow from only one of the four sprinkler heads in the area.

Laboratory testing determined that for the three sprinkler heads which did not actuate, there was no existing flaw and the three heads were physically capable of responding if actuation was required. The actuated sprinkler head successfully extinguished the cable tray fire.

The time sequence of the fire event is summarized in Table 1.

Table 1
Time sequence of the fire event.

Time	Event
t_0	The main control room (MCR) received a fire alarm for the heater bay area. The on-site fire brigade leader was sent to the area to assess the situation.
t_0+10 min	Based on observations at that time, the fire brigade leader reported no fire or smoke, but a steam leak.
t_0+30 min	The unit was switched to another mode per operating procedure; the MCR was unaware at this time of the exact source of the steam leak. It was anticipated that allowing steam to the main turbine and rolling the turbine would assist in mitigating the observed steam leak.
t_0+34 min	The MCR received numerous unexpected alarms and observed other anomalous indications on the MCR panels.
t_0+35 min	Based on these alarms and indications, and since there was a known steam leak, the unit was manually scrammed.
t_0+39 min	In response to field operator reports that sparks had been observed in the building ground floor hallway, the MCR operators actuated the plant fire siren and sent on-site fire brigade leaders.
t_0+44 min	The main steam isolation valves were closed, isolating the steam leak.
t_0+47 min	The MCR received a report that smoke was now observed at the hydrogen seal oil vacuum pump breaker cubicle in a motor control center.
t_0+53 min	The east side of the turbine Fire Alarm System alarmed caused by the actuation of the fire suppression system (a fusible link sprinkler). The fire was extinguished by the automatic sprinkler system.

3. Benchmark methodology

Contrary to a well-controlled experiment, a real fire event does not occur under laboratory conditions and thus only few data are available. Assessing the quality of numerical results simulating such an event is therefore highly challenging. Based on the principle that a code-to-code comparison of simulation results is still possible, a three-step methodology has been developed.

The first step (Step 1) consisted of a calibration phase of the cable fire models on the CFS-2 cable fire test [4] performed within the PRISME 2 project, i.e. in simulating a well-controlled fire scenario for which the entire experimental data and uncertainties are available and provided to the participants. The choice of the CFS-2 test is based on the cable type (PVC insulated

cables) and the ventilation renewal rate (15 h^{-1}) as close as possible to the real fire event characteristics. The second step (Step 2) consisted of a blind simulation of the CFP-D1 cable fire test [7] performed within the PRISME 3 project. Only the input data on the experimental conditions were accessible to the participants and the CFP-D1 test was planned to be carried out after the due date of the blind simulations. The CFP-D1 test satisfies the ventilation renewal rate as closely as possible to the real fire event characteristics but not the type of cables (use of halogen free flame retardant cables (HFFR) in the CFP test campaign). Finally, the last step (Step 3) consisted in performing a real fire event simulation on the basis of the available information recorded in the FIRE Database and the additional information gathered by the national coordinator of the concerned country with support of the licensee [8].

The fire source involved in the real event is very different from what is usually investigated in the PRISME projects. Knowledge on this specific fire source is insufficient, based on the past experiments. In order to bring knowledge on the specific fire source involved in the real fire event and in order to re-calibrate the cable fire models for the event-like fire source between Step 2 and Step 3, an intermediate step (Step 2_2) between Step 2 (renamed Step 2_1) and Step 3 was introduced in the Benchmark Exercise. Step 2_2 consisted of simulating the PRF BCM-S2 test carried out in the SATURNE facility of IRSN (Institut de Radioprotection et de Sûreté Nucléaire) as part of the specific test for the benchmark needs.

The benchmark methodology is based on the fact that a similar behaviour is expected between Step 1 and Step 2_1 and between Step 2_2 and Step 3, making it possible to transpose the error increment ($\Delta\varepsilon$). The goal of the Benchmark Exercise is to assess the behaviour of fire models. It fundamentally means that our own capability in understanding what happens in a real fire event should be necessarily de-correlated from this assessment. It includes the potential false input data, going beyond the usual user bias, selected by the user to perform the simulation. By evaluating the error increment from Step 1 to Step 2_1, both characterized by well-known input conditions, i.e., fire and confined and ventilated (CV) environment, it is solely the additional error due to the blind condition and slightly different configuration that would be taken into account.

A schematic of the 3-step methodology of the Benchmark Exercise is shown in Fig 3.

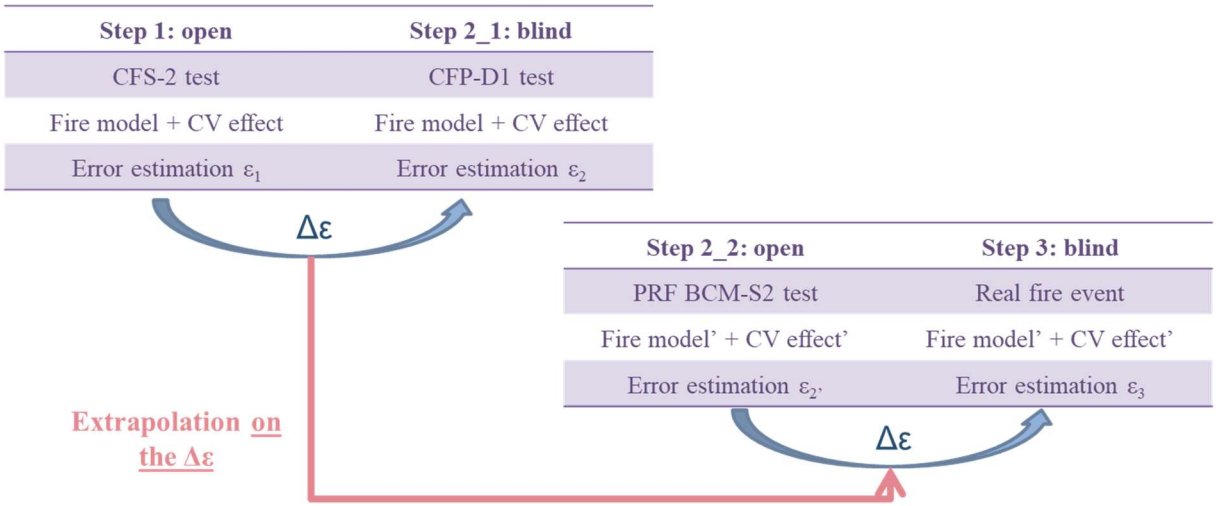

Fig 3. Schematic of the 3-step methodology of the Benchmark Exercise.

Quantifying the capabilities of fire models can be made by using metric operators as suggested by the ASTM E1355-12(2018) [9]. The mathematical methods depend on the characteristics

of the data studied, and a distinction is made between single point comparison, steady-state comparison, and time-dependent values.

For a single point comparison, the data do not depend on time nor space. It is typically a peak value. In this case, the quantitative comparison can be made using an absolute or relative difference. The normalized relative difference "Local_Max_Norm" seems to be appropriate. It accounts for the initial state of the calculation as a reference state to avoid any unit troubles. It is called the local error and expressed as follows:

$$\varepsilon_{local\_max} = \frac{\max[y(t_i)-y(t_0)]-\max[x(t_j)-x(t_0)]}{\max[x(t_j)-x(t_0)]} \quad (1)$$

where "x" is the reference value and "y" the computational one. "$x(t_0)$" and "$y(t_0)$" are the initial values.

For time-dependent values, the simulation results are compared to the experimental values over the fire scenario duration. However, in the frame of a Benchmark Exercise, the numerical results are compared to the experimental values over the common simulated period by the participants. The difference is called the global error and is defined as the normalized Euclidean distance between two vectors (L2_Norm_Index) and expressed as follows:

$$\varepsilon_{global} = \frac{\|\vec{y}-\vec{x}\|}{\|\vec{x}\|} = \sqrt{\frac{\sum_{i=1}^{n}(y_i-x_i)^2}{\sum_{i=1}^{n}(x_i)^2}} \quad (2)$$

Obviously, metrics can be used to conduct both code-to-experiment and code-to-code comparisons. For blind simulations, simulation results are compared to the mean simulation results, obtained by calculating the average values from all the simulations.

4. Overview of the fire simulations

Thirteen institutions from 9 countries (Belgium, Finland, France, Germany, Japan, Korea, Spain, the United Kingdom and the United States of America) participated in this Benchmark Exercise. Simulations were performed using computational fluid dynamics codes (CFD), a lumped-parameter code (LP) and zone codes (ZC). Most of CFD simulations were performed with the FDS software (10 out of 12). Details are reported in Table 2.

Cable tray fire modelling remains a complex issue. Given the multitude of parameters involved in the definition of such a fire source (cable orientation, cable length, number of cable trays, spacing between trays, cables loading, flame retardant compounds, etc.), no theory has yet been put forward on how to model all the aspects of the problem, even for simple, open atmosphere conditions. Some approaches in the form of experimental studies [10],[11] and more recently [3],[4],[7] have nevertheless been carried out and an empirical model referred to as FLASH-CAT [11] (short for flame spread over horizontal cable trays) was developed by the NIST for horizontal cable tray fires in open atmosphere. FLASH-CAT is a relatively simple model for predicting the growth and spread of a fire within a vertical stack of horizontal cable trays.

Hypotheses used by the FLASH-CAT model suggest that the fire should propagate upward through the cable trays depending on an empirical timing sequence only based on the tray order in the stack model and assumes that, once ignited, the cables burn over a length that is greater than that of the tray below. The burning pattern has therefore an expanding V-shape as there is

an increasing length of cable that initially ignite when fire propagates upwards and due to lateral propagation of fire. As the mass of combustible material at the center of the V is consumed, a horizontal extinction front appears at the center of the trays and the V-shape becomes an open wedge until the full length of cable is burnt. The model parameters indicated in [11] have been chosen based on the observation of tests performed at Sandia National Laboratories in very particular conditions.

Most of the participants used a FLASH-CAT-like approach by adapting the original model to compartment fires. Indeed, fires in confined and ventilated compartments often lead to a significant decrease in mass loss rate (MLR), and thus in heat release rate (HRR), compared to the one obtained in open atmosphere. This decrease is mainly due to the reduced heat transfer from the flame to the fuel surface as the oxygen is depleted in the room, because of the air renewal rate that can be quite low compared to the kinetics of oxygen consumption by the fire source. In addition, in a confined enclosure, the flame spread velocity along the cable trays is not constant, unlike in the open atmosphere. Indeed, the increase in temperature of the gas surrounding the cables tends to increase the flame spread velocity while the decrease in oxygen content at the level of the cables tends to reduce this velocity.

Others used a macroscopic model, denoted "Mass loss-based model," which allows for the estimation of the HRR of a cable tray fire knowing some parameters, generally calibrated by comparing the model to real scale experiments available in the literature. From general observations of real scale cable tray fire experiments, a conservative HRR curve is built. This curve being conservative in open conditions, an oxygen limiting law is then used to account for the effect of the confinement.

Table 2
List of benchmark participants

Code type	Institution (Country)	Software	Cable tray fire model
CFD	U-CANTABRIA/CSN (Spain)	FDS v6.7.0	FLASH-CAT-like model
	IRSN (France)	CALIF^{3}S-ISIS v5.3.0	FLASH-CAT-like model
	NRA (Japan)	FDS v6.7.0	Mass loss-based model
	LCPP (France)	FDS v6.7.1	FLASH-CAT-like model
	NRC (United States)	FDS v6.7.1	FLASH-CAT-like model
	iBMB (Germany)	FDS v6.7.1	Mass loss-based model
	VTT (Finland)	FDS v6.7.1/3	FLASH-CAT-like model
	KAERI (Republic of Korea)	FDS v6.7.1	FLASH-CAT-like model
	BEL V (Belgium)	FDS v6.7.1	Mass loss-based model
	EDF (France)	SATURNE v5.2	Mass loss-based model
	ONR (United Kingdom)	FDS v6.7.1/4	FLASH-CAT-like model
	GRS (Germany)	FDS v6.7.1	FLASH-CAT-like model
LP	GRS (Germany)	COCOSYS v3.0	Mass loss-based model
	IRSN (France)	SYLVIA v10.0	FLASH-CAT-like model

ZC	CRIEPI (Japan)	BRI2-CRIEPI v1.0	FLASH-CAT-like model
	EDF (France)	MAGIC v4.1.4	FLASH-CAT-like model

5. Step 1: calibration phase on the PRISME 2 CFS-2 test

5.1 Overview of the CFS-2 test

The PRISME 2 CFS-2 test [4] was carried out in the large-scale fire test DIVA facility of IRSN (see Fig. 4).

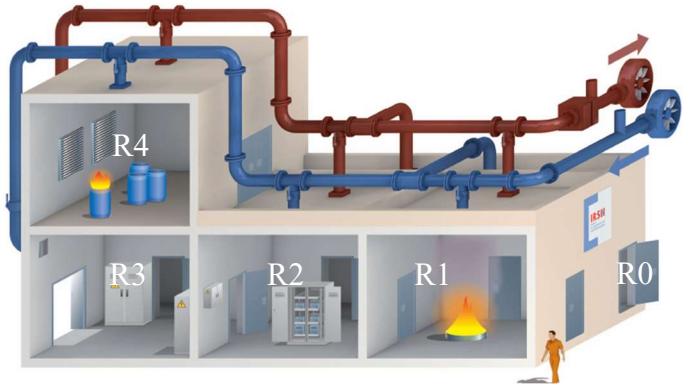

Fig. 4. Perspective view of the DIVA facility of IRSN.

The CFS-2 test only involved rooms R1 and R2. These rooms communicate through a doorway (0.79 m wide x 2.17 m high), as shown in Fig. 5. The fire source was located against the west wall of R1 and was composed of five horizontal ladder-type trays 3 m long, 0.45 m wide and spaced from each other by 0.3 m. Each tray was filled with 32 segments of a 2.4 m long PVC insulated cable. The cable samples were packed loosely along the five trays. In addition, the five trays were set up against an insulated side wall. Ignition was achieved by means of a propane gas burner providing an ignition source of 80 kW. It was located 0.2 m below the lowest cable tray. The ignition source was stopped when the HRR exceeded 400 kW, considering that for such a value (five times higher than the fire power of the gas burner) the cable tray fire source was ignited. The air inlet was located in the upper part of the fire room while the outlet was set up in the upper part of the adjacent room (see Fig. 5). The air renewal rate before ignition was 15 h^{-1}.

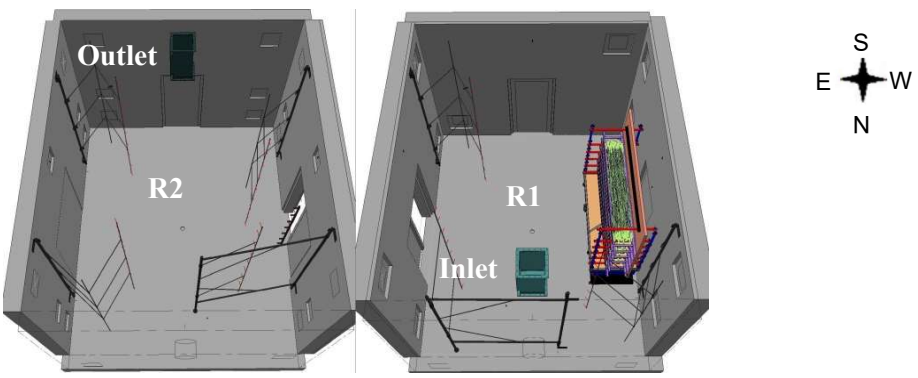

Fig. 5. Schematic of the experimental set-up of the CFS-2 test.

5.2 Analysis of the outcomes of fire simulations

The quantities studied in the Benchmark Exercise are those of major importance in fire safety studies, i.e., HRR, MLR, compartment pressure, gas temperatures and smoke. Only the results for the HRR are shown in this paper for the first two steps. HRR is an essential quantity from which other quantities are deduced.

The experimental and simulated development of the fire HRR over time is plotted in Fig. 6 and the local and global errors on the HRR are indicated in Fig. 7 and Fig. 8, respectively. As most of the CFD simulations were performed with the FDS software, green and blue colors are used to easily identify the FDS results on the graphs. For information purposes, the accuracy of the experimental HRR measurement is 15% [4].

The CFS-2 test was carried out with a high room air renewal rate (15 h^{-1}). The total mass loss (77 ± 2 kg) is identical to that obtained in open atmosphere (77 ± 1 kg) [4]. The under-ventilation of the fire source led to a significant production of unburned hydrocarbons and to their combustion in the upper part of the fire room. The HRR peak reached before the combustions of the unburned gases is 0.8 MW, against 2.7 MW in open atmosphere.

As illustrated in Fig. 6, the predictive simulations of the fire HRR of the CFS-2 test are within the same range except one, particularly keeping in mind that predictively simulating cable tray fires in a confined atmosphere is quite a difficult task. The local error on the HRR peak is predicted within a range from -30% up to +53%, with a mean error of -11% and a standard deviation of ± 9% (see Fig. 7). The global error calculated over the common simulated period ranges between 32% and 91%, with a mean error of 52% and a standard deviation of ± 9%, as shown in Fig. 8.

Several explanations for the deviations from the experimental curve have been put forward. (1), the under-oxygenation of the fire source is taken into account in the simulations by applying a correction factor to the MLR. Depending on the oxygen limiting law used, more or less significant deviations on HRR can be observed. (2), in a confined enclosure, the flame spread velocity along cables is not constant. The burning surface of cables strongly depends on the position of the flame front along the cables. Depending on how the participants accounted for the effect of oxygen depletion and gas temperature on the flame spread velocity, deviations on HRR can be observed. (3), the setup of the cable trays against an insulated side wall contributes to a lower heat removal in the vicinity of the cables, leading to a decrease of the pre-heating time of cables. This wall is not modelled in zone codes (zone code limitation). (4), the CFS-2 test led to a significant production of unburned hydrocarbons in excess and to their fast combustion in the upper part of the fire room due to fresh air provided by the mechanical ventilation. These instabilities of combustion temporarily increased the HRR, as shown in Fig. 5. They were not simulated by the participants.

The calibration of cable fire models on a fire test carried out in a confined and mechanically ventilated environment remains a complex task due to physical phenomena linked to the confinement of the fire source (oxygen depletion, rise in gas temperature, possible occurrence of fast combustion of unburned gases, etc.). No one addressed the problem in the same way.

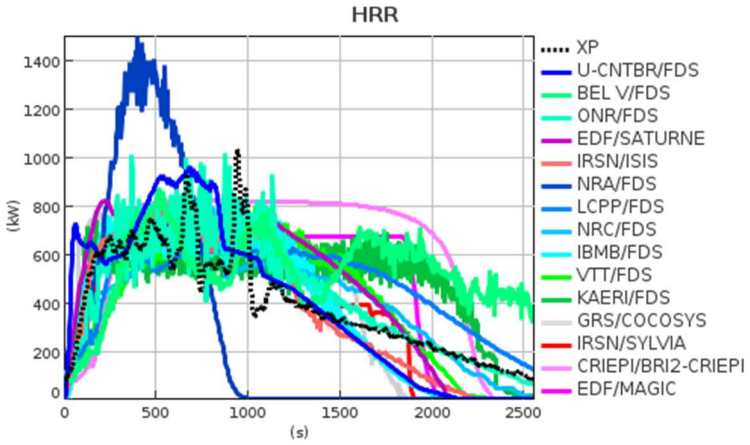

Fig. 6. Simulation results of the HRR for Step 1 compared to the CFS-2 experimental result.

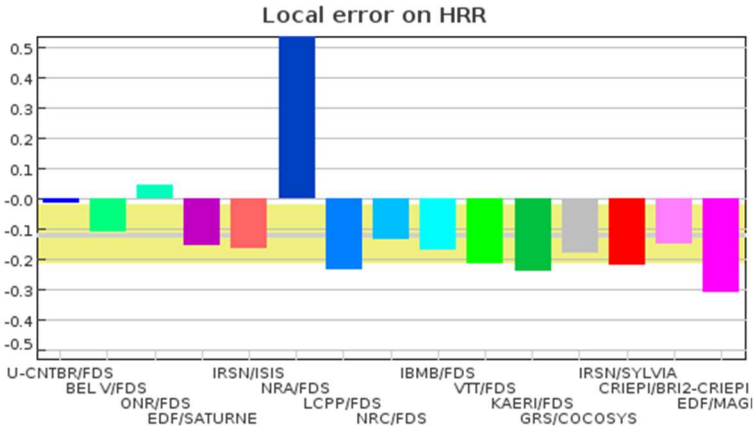

Fig. 7. Local error on HRR for the simulations of Step 1.

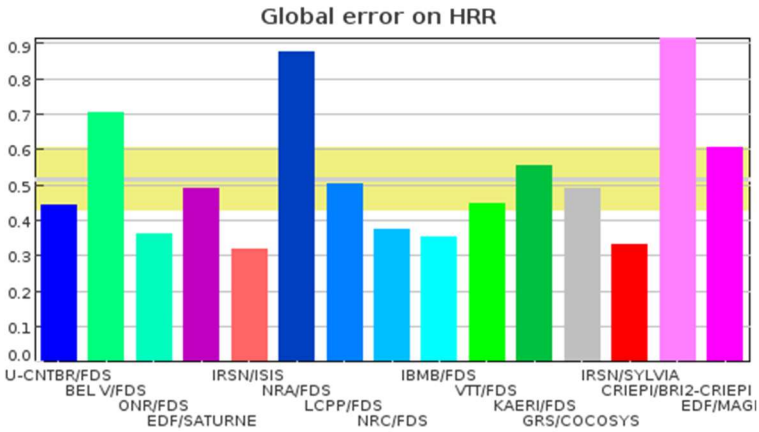

Fig. 8. Global error on HRR for the simulations of Step 1.

6. Step 2_1: blind simulations of the PRISME 3 CFP-D1 test

6.1 Overview of the CFP-D1 test

The CFP-D1 test [7] was selected for the blind simulations of the Benchmark Exercise Step 2_1. The experimental setup of this test is close to that of the CFS-2 test, as illustrated in Fig. 9. It involved rooms R1 and R2 of the DIVA facility connected by a doorway.

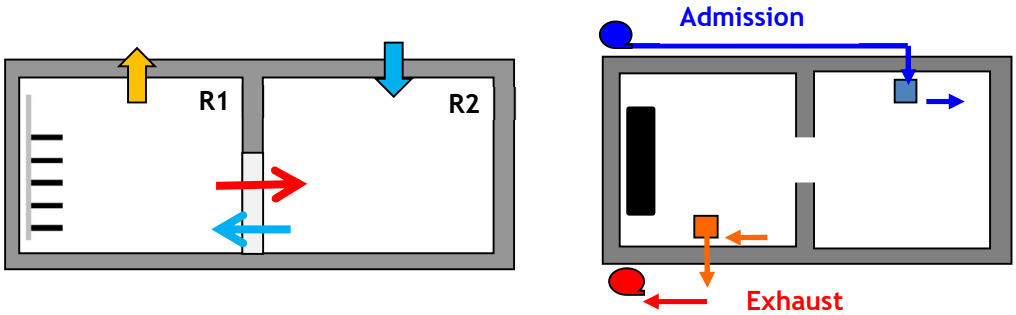

Fig. 9. Schematic of the experimental set-up of the CFP-D1 test.

The CFP-D1 test differs from the CFS-2 test used for the calibration phase by the nature of the cables tested and the gas flow pattern. In the CFS-2 test, the air inlet was located in the upper part of the fire room while the outlet was set up in the upper part of the adjacent room (see Fig. 5). In the CFP-D1 test, the flow pattern is reversed, with an air inlet in the upper part of the adjacent room and an outlet in the upper part of the fire room (see Fig. 9).

The CFP-D1 test was carried out with 5 horizontal cable trays loaded with halogen-free flame retardant (HFFR) cables set up against an insulated side wall, while PVC insulated cables were used in the CFS-2 test. Depending on the nature of the compounds used in flame retardants, a different behaviour of the flame retardant with respect to the fire is observed. Halogens contained in PVC insulated cables mainly act by the action of hydrogen chloride, capturing the hot flame radicals and leading to the flame poisoning [12]. Their efficiency is shown by a reduction of the combustion rate which also depends on external factors, such as the oxygen diffusion rate in the reactive zone or the heat transfer rate from the flame to the surface area of the polymer.

The number of mineral compounds used as flame retardants is relatively small since they have to be decomposed at a relatively low temperature, which is not common for minerals. Alumina trihydrate ($Al(OH)_3$) is one of the most common mineral flame retardant used in HFFR cables because it is inexpensive and easy to incorporate into plastics. Alumina trihydrate is decomposed in a temperature range between 180 °C and 200 °C, as follows:

$$2\ Al(OH)_3 \rightarrow Al_2O_3 + 3\ H_2O\ \ (+\ 298\ kJ/mol) \qquad (3)$$

Alumina trihydrate is cooled by the reaction of dehydration (endothermic reaction), which involves less volatile products released by the combustible. Moreover, aluminum oxide forms a crust at the cable surface, which protects against subsequent degradation of the material. Finally, water vapor released by the dehydration reaction dilutes the gaseous phase and decreases the amount of oxygen at the cable surface.

In terms of modelling, the effect of mineral compounds used as flame retardants on the combustion of cables is taken into account in the cable thermal inertia term (0.27 kW^2s/m^4K^2

for PVC insulated cables tested in the CFS-2 test against 0.90 kW^2s/m^4K^2 for HFFR cables tested in the CFP-D1 test). This results in a delay in the heat up of the cable surface and a slower flame spread velocity compared to PVC insulated cables.

6.2 Analysis of the outcomes of fire simulations

The experimental and simulated development of the fire HRR over time is plotted in Fig. 10 and the local and global errors on the HRR are indicated in Fig. 11 and Fig. 12 respectively. No results with the EDF MAGIC code are available for this step and the next steps.

As for the CFS-2 test, the CFP-D1 test was carried out with a high room air renewal rate (16 h^{-1}). The total mass loss (116 kg) is of the same order of magnitude as that obtained in open atmosphere (97 ± 7 kg) [3]. The ventilation layout significantly influenced the fire HRR. Indeed, the HRR peak reached 1.8 MW in the CFP-D1 test, against 2.2 MW in open atmosphere and 1.3 MW in the PRISME 2 CFS-4 test [3] carried out with the same type of fire source but with the gas flow pattern of the CFS-2 test. The ventilation layout of the CFP-D1 test led to better oxygenation of the fire source by fresh air coming from the open doorway between the two rooms. The production of unburned hydrocarbons was low. The maximum concentration in the fire room reached 5,000 ppm.

Most of the simulations underestimated the HRR peak as shown in Fig. 10, except those of BELV and VTT which correctly predicted the peak value with two different approaches of the cable tray fire modelling (cf. Table 2). Differences from one simulation to another may be large, resulting in wide error ranges, which reflects the difficulty in modelling such a fire source in a confined and mechanically ventilated atmosphere, even with a calibration of the models, and the difficulty in correctly predicting gas flows in the fire room for such a complex fire source.

The local error on the HRR peak is predicted within a range from -68% up to +81%, with a mean error of -23% and a standard deviation of ±19% (see Fig. 11). The global error calculated over the common simulated period ranges between 18% and 102 %, with a mean error of 54% (47% for the comparison with the mean simulation result) and a standard deviation of ±12%, as shown in Fig. 12. Thus, the code-to-experiment comparison for the HRR led to a slightly higher mean global error compared to the code-to-code comparison.

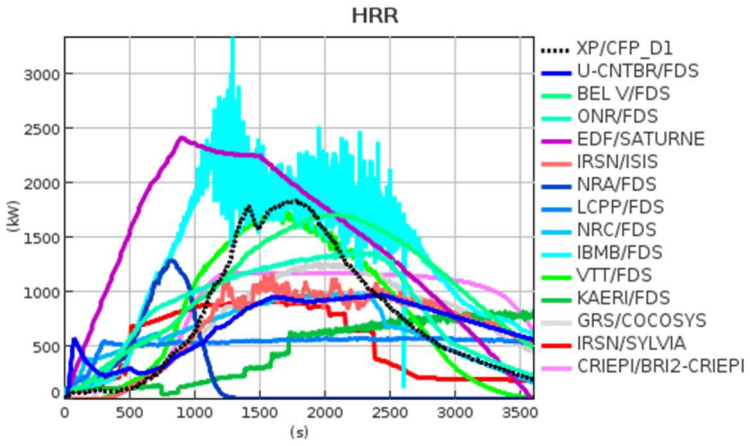

Fig. 10. Blind simulation results of the HRR for Step 2_1 compared to the CFP-D1 experimental result.

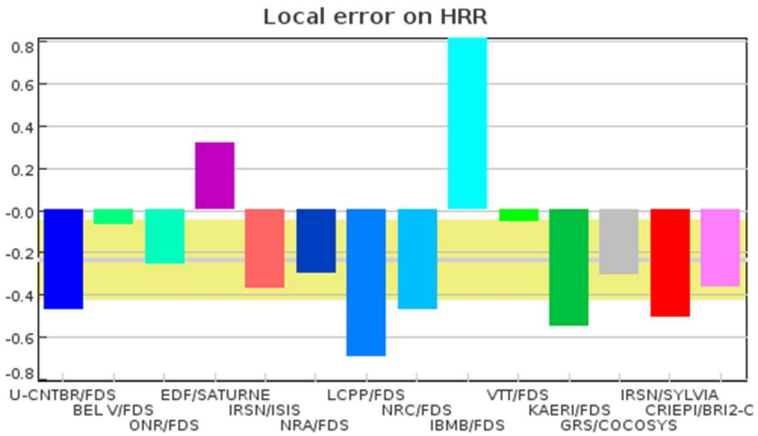

Fig. 11. Local error on HRR for the blind simulations of Step 2_1 compared to the CFP-D1 experimental result.

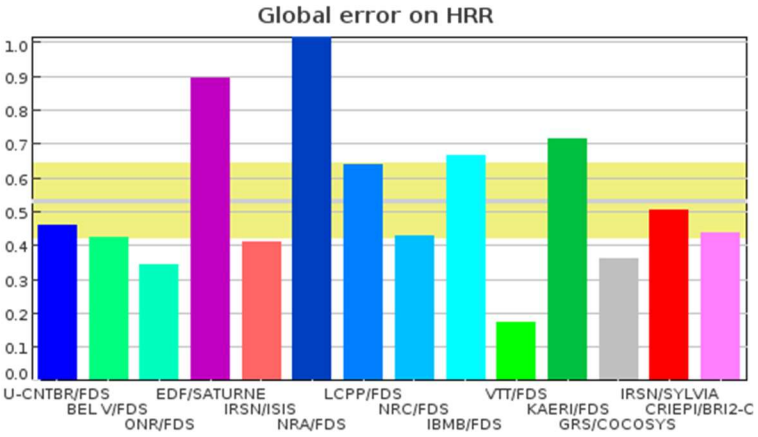

Fig. 12. Global error on HRR for the blind simulations of Step 2_1 compared to the CFP-D1 experimental result.

6.3 Error increment from Step 1 to Step 2_1

Recall that the benchmark methodology is based on the fact that a similar behaviour is expected between Step 1 and Step 2_1 and between Step 2_2 and Step 3, making it possible to transpose the error increment.

The variation of local and global errors on the HRR from Step 1 to Step 2_1 is shown in Fig. 13 and Fig. 14 respectively.

The local error variation on the HRR peak from Step 1 to Step 2_1 is predicted within a range from -83% up to +97%, with a mean error of -14% and a standard deviation of ±21% (see Fig. 13). The global error variation calculated over the common simulated period ranges between -48% and +41%, with a mean error of +2% and a standard deviation of ±11%, as shown in Fig. 14).

For most of the simulations, the error increment on the global error is positive as expected. However, the low value in the global error increase for HRR (+2%) would suggest that the HRR trend prediction in blind conditions for a well-known fire has a quality similar to that of an open case.

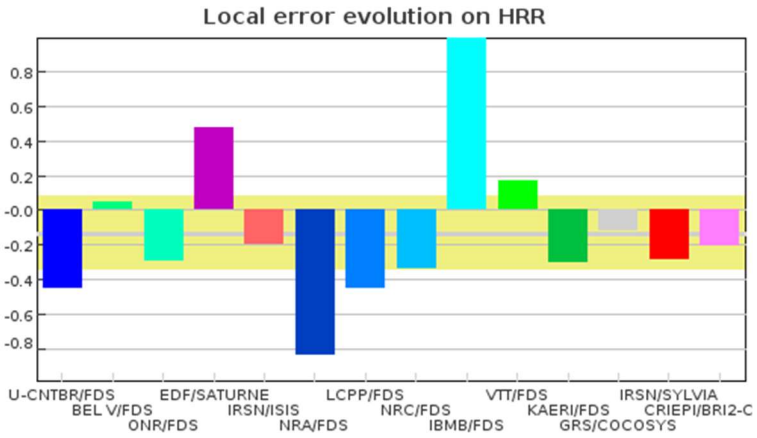

Fig. 13. Local error variation on HRR from Step 1 to Step 2_1.

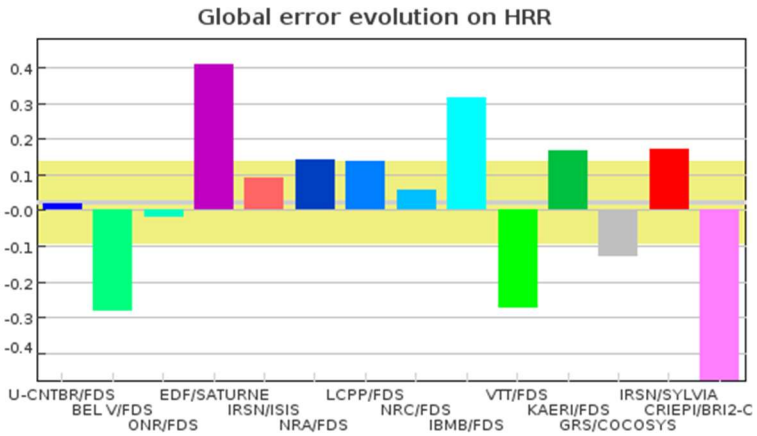

Fig. 14. Global error variation on HRR from Step 1 to Step 2_1.

7. Step 2_2: open simulations of the PRF BCM-S2 test

7.1 Overview of the PRF BCM-S2 test

The PRF BCM-S2 test is the specific test carried out in order to bring knowledge on the specific fire source of the real fire event and to re-calibrate the fire models on the event-like fire source between Step 2 and Step 3.

This test was conducted under the large-scale calorimetric hood in the SATURNE facility of IRSN (10 m long, 10 m wide and 20 m high, see Fig. 15), considering that oxygen depletion is assumed to be weak in the real fire event. The smoke exhaust hood has a square cross-section of 4.5 x 4.5 m^2. It is connected to the exhaust duct of a ventilation network equipped with a dilution line, high efficiency particulate air (HEPA) filters and fans. The aspiration volume flow rate of the calorimetric hood is about 26,000 $m^3.h^{-1}$. The measurements allow the determination of the fire heat release rate considering both the oxygen consumption and the carbon dioxide generation methods. The exhaust duct contains a measurement duct devoted to the smoke characterization. Many openings are located at the top of the SATURNE facility on

each of the four sides. They provide enough air to maintain the oxygen concentration at 21% in the vicinity of the fire source, as in open atmosphere.

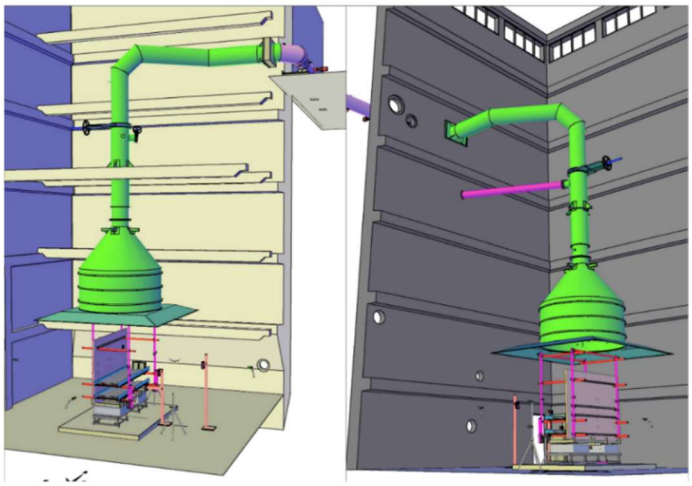

Fig. 15. Schematic of the calorimetric hood in the SATURNE facility.

A simplification for the cable information for the simulation of the real fire event was proposed by U.S. NRC so that benchmark participants can operate with known generic properties for the testing and modelling work. The starting point was the THIEF (Thermally-Induced Electrical Failure) [13]. Thus, simulations of the heater bay fire event were performed with PE/PVC (Polyethylene/Polyvinyl chloride) insulated cables as the ones supplied by U.S. NRC and tested in the PRF BCM-S2 test.

The fire source consists of two horizontal cable trays similar to the cable trays involved in the heater bay fire event, as illustrated in Fig. 16. The tray dimensions are 900 mm in width, 3000 mm in length, and 150 mm in height. The distance between trays is 450 mm. The cable trays are ladder-type cable trays, open on the bottom side. Rungs are arranged every 300 mm and measure approximately 25 mm. The two-cable-tray stack is set up against an insulated side wall (2600 mm in length, 2200 mm in height and 40 mm in depth). The side wall consists of a panel of insulated material (Superwool 607 HT Board) attached to a metallic frame with angle bars.

Each tray is filled with 112 PE/PVC insulated cable samples (15.9 mm in diameter, 2.4 m-long). The cables are set loosely in the trays with a height filling rate corresponding to approximately half the height of the tray and, consequently, half the cable depth of the real fire event.

In order to reproduce the real fire event as closely as possible, the cable ignition in the PRF BCM-S2 test is achieved by means of two couples of blowtorches, one located below the upper cable tray and directed upwards and the other, above the lower cable tray and directed downwards, as illustrated in Fig. 16. The blowtorches are located at the center of the trays and near the sidewall. Each blowtorch couple provides a power source of about 6.5 kW (0.15 $g.s^{-1}$ of propane) for 2 min and 30 s, then the power is increased to 9 kW (0.2 $g.s^{-1}$) to ensure ignition.

The blowtorch flame forms a tube (15 mm in diameter, 100 mm in length) touching the cables. The temperature of the jet flame ejected from the blowtorch is about 1200°C and is comparable to the melting temperature of copper (1085°C) as it probably happened in the event with the arc fault. The blowtorches were stopped after 760 s (12 min 40 s).

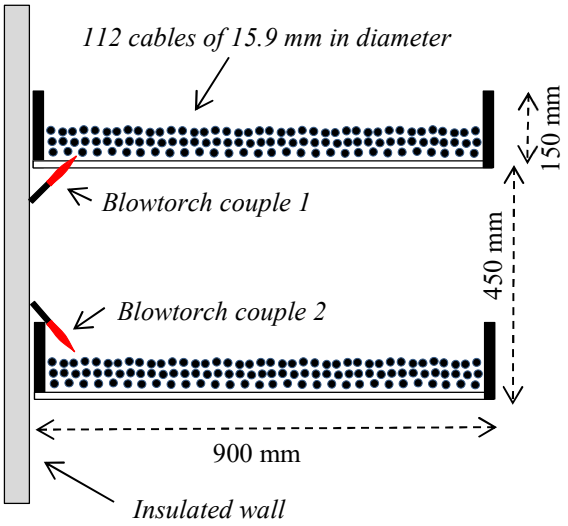

Fig. 16. Scheme of the PRF BCM-S2 test fire source.

The composition of the cables and their burning characteristics are reported in Tables 3 and 4 respectively. For the FLASH-CAT-like modelling, the average bench-scale heat release rate per unit area under 50 kW.m^{-2} irradiance is 245 kW/m^2 and 314 kW/m^2 under 75 kW/m^2 irradiance. Since the cable's thermal inertia and ignition temperature were not available, values of 0.27 kW^{2}s/m^{4}K^2 for the thermal inertia and 218 °C for the ignition temperature were suggested according to PVC insulated cables tested in the CFS-2 test.

Table 3
Composition of the cables.

Insulation material	PE
Jacket material	PVC
Conductors	7
Diameter [mm]	15.9
Jacket thickness [mm]	1.85
Insulator thickness [mm]	1.07
Mass per length [kg/m]	0.38
Copper mass fraction [–]	0.55
Jacket mass fraction [–]	0.27
Insulation mass fraction [–]	0.10
Filler mass fraction [–]	0.08

Table 4
Burning characteristics of the cables.

Y_{CO2} ($g.g^{-1}$)	Y_{CO} ($g.g^{-1}$)	Y_{CnHm} ($g.g^{-1}$)	Y_{soot} ($g.g^{-1}$)	Y_{Hcl} ($g.g^{-1}$)	ΔHc ($MJ.kg^{-1}$)	Radiative heat fraction (-)
1.60	0.11	0.08	0.03	0.03	24	0.35

C_nH_m: unburned hydrocarbons. Yield of a species i (Y_i) is defined as the ratio of the total cumulative mass of species i produced to the total mass loss of the combustible.

7.2 Analysis of the outcomes of fire simulations

The experimental and simulated development of the fire HRR over time is plotted in Fig. 17 and the local and global errors on the HRR are indicated in Fig. 18 and Fig. 19 respectively.

In accordance with the power delivered by the blowtorches, the incubation stage of the fire lasted for 620 s. This time corresponds to the preheating time of the cables. Then, a fast increase in the HRR was observed, with a HRR peak of 2.3 MW reached in a few minutes and corresponding to the fast spreading stage of the fire. The two blowtorches directed towards the bottom of the upper tray induced a ceiling flame regime for approximately 10 minutes, which favored the preheating of the cables of the lower tray. After the HRR peak, the fire HRR decreased progressively until fire extinction. During the decay stage of the fire, small increases in HRR were observed, as shown in Fig. 17. According to a video analysis, these peaks are correlated with the flame color changes (soot effect).

The low power ignition protocol over a longer time as used in the PRF BCM-S2 test led to a better preheating of the cables and a higher fire growth rate compared to a conventional ignition of cables with a sand burner located below the lower cable tray and delivering a power source of 80 kW as used in a second test, the PRF BCM-S1 test, for the same type of fire source under the the calorimetric hood in the SATURNE facility.

The predicted HRR peak is captured by the models for most of the participants. Deviations from the experimental values are nevertheless observed on the duration of the incubation stage of the fire, showing the difficulty of correctly predicting the preheating of the cables. The lack of data on the cable thermal inertia and cable ignition temperature contributed to these deviations when preheating was calculated, since these quantities play an important role in the preheating time of cables. It is important to capture the incubation stage of the fire with this specific ignition power because in the heater bay fire event, the actuation of the automatic sprinkler system prevented the full development of the fire.

The local error on the HRR peak is predicted within a range from -44% up to +52%, with a mean error of -4% and a standard deviation of ±12% (see Fig. 18). The global error calculated over the common simulated period ranges between 15% and 144%, with a mean error of 58% and a standard deviation of ±18%, as shown in Fig. 19. No results from CRIEPI and ONR are available for this step.

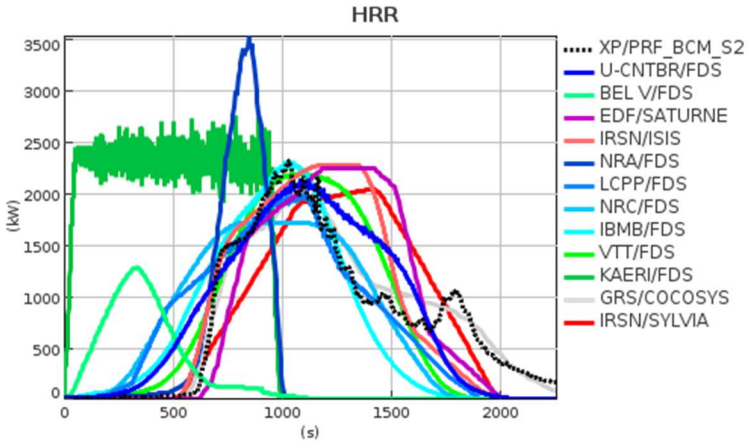

Fig. 17. Simulation results of the HRR for Step 2_2 compared to the BCM-S2 experimental result.

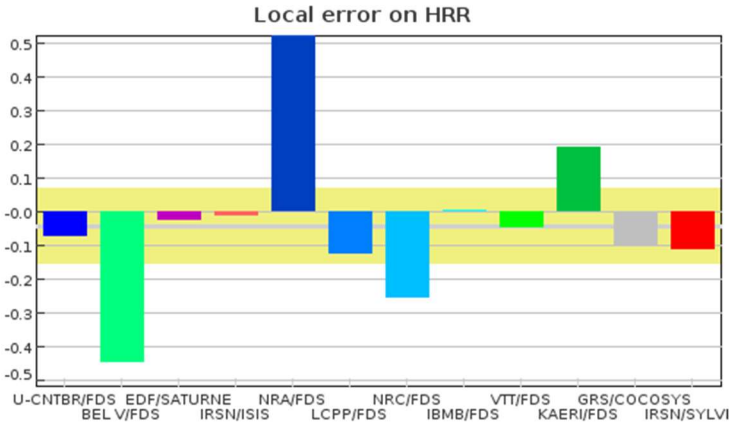

Fig. 18. Local error on HRR for the simulations of Step 2_2.

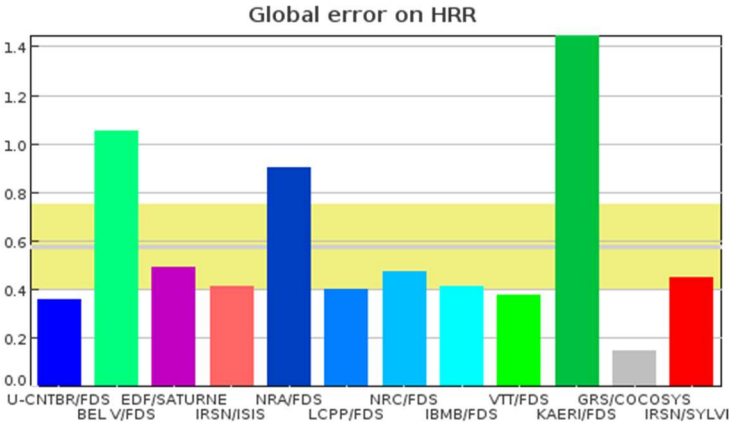

Fig. 19. Global error on HRR for the simulations of Step 2_2.

7.3 Error estimation on HRR for Step 3

Since no data on the fire development of the heater bay fire event is available, as it is a real fire event, the error estimation for step 3 is based on the fact that a similar behaviour is expected between Step 1 to Step 2_1, and Step 2_2 to Step 3, making it possible to transpose the error increment.

The estimated local and global errors on the HRR for step 3 are indicated in Fig. 20 and Fig. 21 respectively. The local error on the maximum value of the HRR ranges from -59% up to +98%, with a mean error of -15% and a standard deviation of ±22% (see Fig. 20). The estimated global error on HRR ranges between 1% and 161%, with a mean error of 64% and a standard deviation of ±21%, as shown in Fig. 21.

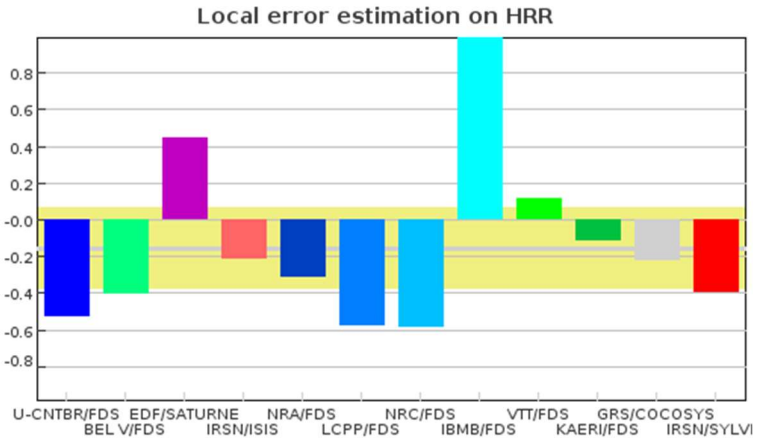

Fig. 20. Local error estimation on HRR for Step 3.

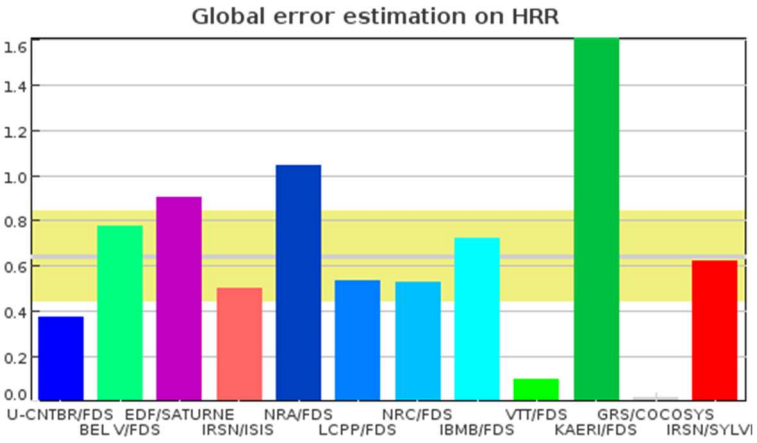

Fig. 21. Local error estimation on HRR for Step 3.

As explained in the methodology, these values on the local and global errors on the HRR peak and on the HRR evolution over time, respectively, represent the confidence that users can have in their simulation tool when addressing a real fire event such as the one of Step 3. The ability of the user to correctly understand an event and set the right parameters for the simulation is another matter that is illustrated in the following section.

8. Step 3: simulations of the heater bay fire event

8.1. Available data and assumptions

Since a real fire event does not occur under laboratory conditions, available data are limited. At the exit point from the upper tray, cables were severed, and the applicable jacket/insulation was removed due to excessive heat. An initial inspection showed localized fire damage in the shape of a semicircle 0.76 m long and 0.51 m wide, as illustrated in Fig. 22. Charring was present throughout the entire depth of cables in that section (approximately 0.15 m deep).

The extent of cable damage in this area included cables severed, cable jacket/insulation damage, cable jacket/insulation completely removed and sections of the cables missing. The most extensive charring and damage was observed on those cables located at the bottom of the upper tray with signs of an arc flash. The initial inspection of the lower tray showed localized fire damage in the shape of a semicircle approximately 1.02 m long and 0.66 m wide, as illustrated in Fig. 22. Charring was present throughout the 0.10 m top of cables in that area. Molten drips could be seen on top of numerous cables on the lower tray (tests subsequently verified that cuprous oxide was present in large quantities on the cables of the lower tray).

Signs of minor concrete spalling were observed on the diagonal concrete overhang located above the affected cable trays. The smoke damage to the wall formed a v-pattern with a wide shape that extended to the ceiling, indicating a slowly burning fire.

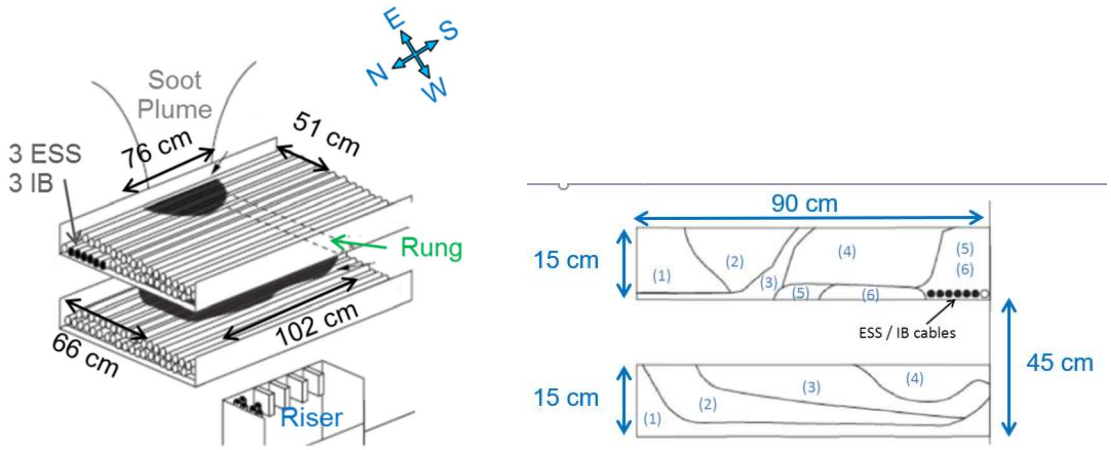

(1) No damage, (2) Moderate damage (partial jacket damage), (3) Medium damage (complete jacket damage), (4) Heavy damage (complete jacket damage with partial insulation wire damage), (5) Extreme damage, (6) Severed cables

Fig. 22. Damage pattern of the cable trays.

A coarse estimation of the fire load involved in the real fire event was done. Details are reported in Table 5. This estimation is based on the assumptions that damage classes 3 to 6 on both cable trays are idealized by a half-truncated cone and that the volume of damage class 2 is located around the larger affected areas. Assuming a raw density of the combustible parts of the cables of 230 kg/m^3 and combustion heat of 24 MJ/kg deduced from the PRF BCM-S2 test results, about 630 MJ energy would have been released by the fire (excluding any electrical heat due to arcing), corresponding to a mass loss of about 26 kg.

The dimensions of the ground of the turbine building including the heater bay are almost the only available data regarding the building geometry as shown in Fig. 23. It is a very large

building of about 1,900 m^2 ground surface with approximately 600 m^2 ground surface for the heater bay. The heater bay is an area of the plant containing high pressure feed-water heaters, pipes, cable trays, risers, and overhangs as shown in Fig. 1. A free volume of 2,900 m^3 is set by default, corresponding to 80% of the estimated physical volume of the heater bay from available data. The heater bay has a mezzanine located at 6.1 m from the ground (see Fig. 2) where the fire occurred. In addition, the heater bay is connected to the rest of the turbine building by several openings, indicated by orange lines in Fig. 23. The riser also creates an opening between the mezzanine level and the ground level, just beneath the fire. The trays' routing and pictures of the event indicate a passage through a hole to the back area of the heater bay. The latter two openings have not been considered in the overall dimensions, but they potentially induced flows in the vicinity of the fire ignition.

According to the fire event sequence (see Table 1) and the statement of the representative of the FIRE member country where the fire occurred, it was concluded that the fire was not affected by the mechanical ventilation since the room's ventilation was isolated by closing of the fire dampers actuated by smoke detection. Therefore, simulations were performed without mechanical ventilation. In addition, the overall pressure rise in the turbine building is likely to be negligible, even with the steam leak. This assumption is based on the small size of the steam pipe (few centimeters in diameter) and the supposed large openings to the rest of the turbine building. Thus, the steam leak was not considered in the simulations, but its effects were nevertheless taken into account through the presupposed initial gas temperature (30 °C) and relative humidity in the compartments (90 %).

Table 5
Coarse estimation of the fire load.

		Upper tray			**Lower tray**		
Damage class	Pyrolyzed fraction (%)	Volume (cm^3)	Mass loss (kg)	Heat loss (MJ)	Volume (cm^3)	Mass loss (kg)	Heat loss (MJ)
2	15	46,186	1.59	38.1	60,691	2.08	49.9
3	50	27,489	3.16	75.8	53,073	6.09	146.1
4	80	37,672	6.92	166.1	10,866	1.99	47.7
5	100	4,199	0.96	23.0			
6	100	5,726	1.31	31.4			
5-6	100	9,558	2.20	52.8			
Total			**16.14**	**387.2**		**10.1**	**243.7**

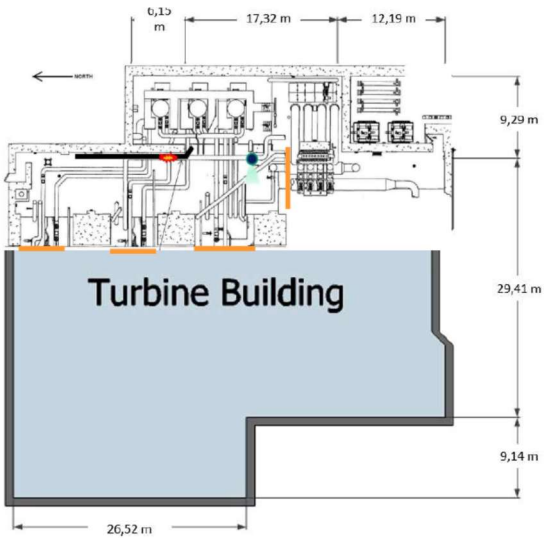

Fig. 23. Scheme of the top view of the turbine building including the heater bay.

As mentioned before, a simplification for the cable information was proposed by the U.S. NRC so that Benchmark participants could operate with known generic properties for the testing and modelling work. Thus, the fire source for the simulation of the real event was equivalent to that of the PRF BCM-S2 test (see Fig. 16).

The fire ignition scenario is very far from scenarios studied in PRISME projects. Fire ignition due to an arc fault is not modeled by fire simulation tools. Therefore, it is assumed that the complete electric power of the defective cables is converted into a localized heat source. Nevertheless, simulating an arc fault by an "equivalent" heat source requires information on the power of cables and the duration of the arc fault. Since these data are not available, default values were set in the simulations. It was suggested to use a power source equivalent to that of the propane sand burner used in the PRISME 2 CFS-2 test for the ignition of PVC insulated cables. It provided a power source of 80 kW for 2 min and 26 sec. It was also suggested to use thermally thick targets to ignite the cables (one in each cable tray). The ignition of cables would then be dominated by a temperature criterion.

Four sprinkler heads (manufacturer reference C-DURASPEED) were located in the vicinity of the fire, at about 1.20 m to 1.50 m above the top of the upper tray, as illustrated in Fig. 24. The sprinkler heads are actuated thermally by fusible links set to break at 100 °C with a standard response time. The heat generated by the fire caused flow from only one of the four sprinkler heads 19 min after the fire detection (cf. Table 1). Since the fire source was located under an overhang below the ceiling of the heater bay, the overhang probably played an important role in the actuation time of the sprinkler.

Fig. 24. Scheme of the spatial arrangement of the sprinkler heads.

8.2 Analysis of the outcomes of fire simulations

According to the time sequence of the event (see Table 1), the beginning time for the simulations (t = 0 s) was set at the event time t_0+34 min, because no indication of fire was reported by the fire brigade before this time.

The benchmark participants were requested to simulate the development of the fire until the temperature criterion of 100 °C was reached at the elevation of the actuated sprinkler, considering that fire extinction will occur when the sprinkler is activated, as in the real fire scenario.

The predicted development of the fire HRR over time is plotted in Fig. 25 and is compared to the mean simulation result over the common simulated period (341 s according to the shortest simulation). Despite this short time, the mean simulation gives an indication of how the ignition of cables has been modelled by the benchmark participants.

The fire growth rates predicted by different codes and users are very different from each other, highlighting the difficulty of predicting the ignition of cables as well as the incubation stage of the fire of such a fire source. For the simulations predicting the triggering of the sprinkler, the predicted HRR just before the actuation of the sprinkler ranges from 290 kW to 2600 kW with most of the predictions below 1000 kW.

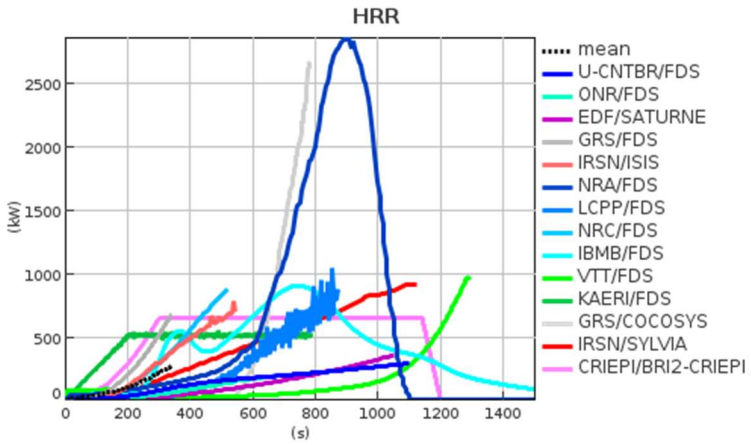

Fig. 25. Simulation results of the HRR for Step 3 compared to the mean simulation result.

One explanation to this observation is that Benchmark participants do not have the same models, nor the same requested input data for the simulation, nor the same approach of choosing them. Differences are also linked to the predictivity level of the simulation tools (i.e., the number of parameters defined by the user compared to the parameter fully predicted from basic data) and from the user choices. The benchmark strategy required to use as far as possible the same input data as from the previous steps and in particular similar input parameters taken from the PRF BCM-S2 test. Even if the intention was to characterize the new configuration through the PRF BCM-S2 test, it must be admitted that the experiment may not be sufficiently representative of the real fire event sequence characteristics (e.g., different type of ignition, time and sequence of ignition and trays loading). Therefore, an important question raised is to what extent the PRF BCM-S2 data are suitable and sufficiently reliable in order to characterise the event.

The phenomenology and observations from the real fire event and the PRF BCM-S2 test are different. Therefore, one open question is how it was possible to receive good results using

strictly all the PRF BCM-S2 data. This again raises the question of the user choices. Which burning surface at ignition should be considered according to the damage picture (cf. Figure 22)? In the PRF BCM-S2 test, cables were burnt along the entire width of the cable tray, which was not the case in the real fire event. This user choice could be shown to play a key role regarding the fire development, even though the other propagation parameters in the FLASH-CAT model remained the same as for the previous steps.

The predictive simulation results of the gas temperature at the elevation of the actuated sprinkler head compared to the mean simulation result are plotted in Fig. 26.

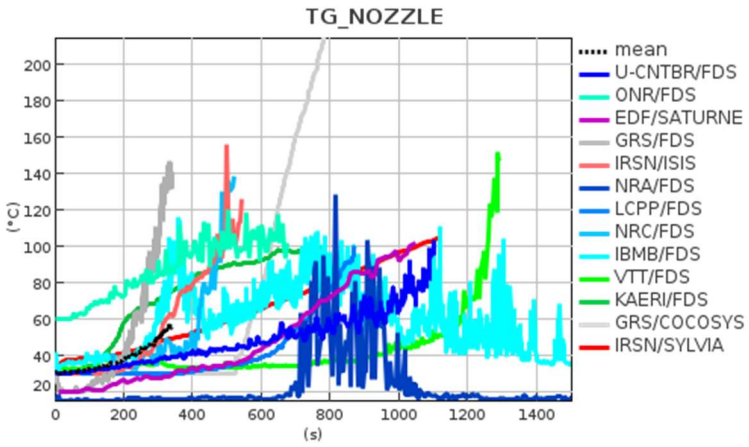

Fig. 26. Simulation results of the gas temperature at the elevation of the actuated sprinkler head compared to the mean simulation result.

The simulations were performed assuming the location of the sprinklers between 1.20 and 1.50 m above the top of the upper tray (50 to 80 cm below the ceiling of the heater bay). The gas temperature at the elevation of the sprinkler heads was the reference temperature used in the simulations for the triggering of the sprinkler.

In most simulations, the critical temperature of 100 °C for the actuation of the sprinkler is reached. Only three simulations out of fourteen do not predict the actuation of the sprinkler. The maximum value of the gas temperature at the sprinkler head location predicted just before actuation ranges from 100 °C to 215 °C. The predicted temperatures above the critical temperature of 100°C are due to the consideration of the response time index (RTI) of the sprinkler head in the simulations. The RTI is a measure of the thermal sensitivity of the sprinkler's heat sensitive element. The exact RTI was not given by the manufacturer because of the age of the sprinklers. It is reportedly 80 $m^{1/2}s^{1/2}$ or greater. Therefore, the RTI was set at 100 $m^{1/2}s^{1/2}$ by default in the simulations.

The predicted actuation time of the sprinkler and the mass and heat losses resulting from the burning of cables are reported in Table 6. For simulations that do not predict the sprinkler actuation, the values reported in the table are those after a fire duration of 60 min (end time of the simulation in this case).

Table 6
Predicted actuation time of the sprinkler and mass and heat losses from the burning of cables.

Institution (Country)	Code type	Software	Sprinkler Actuation Time [min]	Upper Tray Mass Loss [kg]	Lower Tray Mass Loss [kg]	Total Heat Loss [MJ]
VTT (Finland)	CFD	FDS v6.7.1/3	22	3.4	0.5	3501
EDF (France)	CFD	SATURNE v5.2	18	11.6	11.6	371
LCPP (France)	CFD	FDS v6.7.1	15	4.6	3.7	199
IRSN (France)	CFD	CALIF^{3}S-ISIS v5.3.0	9	4.4	2.1	154
IRSN (France)	ZC	SYLVIA v10.0	19	10.0	9.8	466
GRS (Germany)	CFD	FDS v6.7.1	6	1.9	1.0	70
iBMB (Germany)	CFD	FDS v6.7.1	–	16.8	11.0	592
GRS (Germany)	LPC	COCOSYS v3.0	13	7.3	8.0	245
NRA (Japan)	CFD	FDS v6.7.0	–	–	–	–
CRIEPI (Japan)	ZC	BRI2-CRIEPI v1.0	–	16.2	10.1	632
KAERI (Republic of Korea)	CFD	FDS v6.7.1	13	5.3	9.3	350
U-CANTABRIA (Spain)	CFD	FDS v6.7.0	18	3.4	3.4	147
ONR (United Kingdom)	CFD	FDS v6.7.1/4	11	0.9	1.2	51
NRC (United States)	CFD	FDS v6.7.1	9	3.6	2.9	155

The predicted actuation time of the sprinkler ranges between 6 min and 22 min. These times are to be compared to the estimated fire duration i.e., 20 min (± 2 min). Almost all simulations in which the sprinkler is actuated predict a shorter fire duration. The large variation in range highlights the difficulty of predicting such a fire scenario. Indeed, when considering the development of the fire in the inner part of the cable trays involving cables not directly exposed to the (open) flames but surrounded by the outer cables, the presence of an overhang with uncertain dimensions above the cable trays (see Figure 24), potential flows induced by the riser beneath the cable trays and the uncertainty related to the exact position of the actuated sprinkler

head made it difficult to estimate the time of triggering the sprinkler. Short fire durations are obtained if the fire plume rapidly reaches the sprinkler head position. Longer fire durations are obtained if the sprinkler head is not located in the area of the fire plume, thus allowing time for the fire to fill the ceiling with smoke, until the smoke line reaches the sprinkler elevation.

Based on what is known from the event, none of these two situations is the right one. It is likely that, for some reasons already mentioned, the deviation of the flow in the real event from that in the experiment was sufficient to prevent the fire plume from reaching the sprinkler at the very beginning of the fire when the flame was quite weak and therefore more prone to flow disturbances. In contrast, the hypothesis of a regular smoke filling of the ceiling down to the sprinkler elevation would have resulted in the actuation of all four sprinkler heads (which was not the case in the event) in the area, unless the sprinkler head in the direct vicinity of the fire plume had become hotter due to thermal radiation from soot in the fire plume.

In the simulations predicting the sprinkler actuation, the predicted mass loss of the cables in the upper tray just before sprinkler actuation, ranges from 0.9 kg up to 11.6 kg. All predicted values are lower than the coarse estimation from the figure of the damaged areas i.e., 16 kg for the upper tray (see Table 5). However, this value must be taken with caution considering the uncertainties in this estimation. For the lower tray, the predicted mass loss of the cables just before sprinkler actuation ranges from 0.5 kg up to 11.6 kg compared to 10 kg from the coarse estimation. Most of the simulations predict a lower mass loss of the cables in the lower tray compared to that of the upper tray, as observed in the event. Finally, the total heat loss predicted just before sprinkler actuation ranges from 51 MJ up to 3501 MJ, with almost all values below 500 MJ. These values are to be compared to the coarse value of 631 MJ estimated from the figure of the damaged areas.

9. Conclusions

A joint OECD/NEA FIRE and PRISME Cable Benchmark Exercise has been conducted for a realistic cable fire scenario in an electrical system of a NPP. The major goal of this Benchmark Exercise was to simulate a real cable fire event in order to assess the behaviour of fire models for such a complex fire scenario from the operating experience of nuclear installations with the available knowledge.

The event for the Benchmark has been selected from the OECD/NEA FIRE Database thus ensuring the reality of the scenario. Several criteria were applied to select a suitable event from all those recorded in the Database. The predominant criterion was the ability to obtain additional information on the event sequence and characteristics from the licensee. Conducting this Benchmark activity solely based on information contained in the FIRE Database turned out to be not possible, as the available data deal with operating conditions of the plant before and during the fire, the event description and interpretation, safety procedures, root causes identifications, fire detection, fire suppression, and corrective actions.

Various additional data have therefore been provided by the licensee enabling the organisers and participants of the Benchmark Exercise to use the selected cable fire event for Benchmark purposes. The time sequence of the event, the floor dimensions of the turbine building, where the event had occurred, the characteristics of the sprinkler heads close to the fire, and the diagram of the damage caused to the cable trays are almost the only available information for the participants' understanding of the fire scenario.

Nevertheless, it was necessary to carry out a specific cable fire test, named PRF BCM-S2, under the large-scale calorimetric hood in the SATURNE facility of IRSN in order to characterize the fire source despite the knowledge already provided by the PRISME experimental

programs, and to re-calibrate the fire models. Many hypotheses have been agreed among the participants to make up for the remaining unknowns or uncertainties. To some extent, the simulated scenario is, in fact, an event-based scenario from what was understood of the event and what was technically possible to achieve.

The Benchmark Exercise highlighted that cable tray fire modelling remains a complex issue. Given the multitude of parameters involved in the definition of such a fire source, no theory to date has been put forward on how to model all aspects of the problem, even for only open atmosphere conditions. The calibration of the fire models (Benchmark Step 1) on a fire test carried out in a confined and mechanically ventilated environment was a complex task due to physical phenomena linked to the confinement of the fire source (oxygen depletion, rise in gas temperature, possible occurrence of fast combustion of unburned gases, etc.). No one addressed the problem in the same way.

Benchmark Step 2_1 consisted of a blind simulation of a cable fire test performed within the PRISME 3 project. Only the input data on the experimental conditions were accessible to the participants and this test was planned to be carried out after the due date of the blind simulations. The results of the blind simulations showed that the differences from one simulation to another may be large, resulting in wide error ranges, which reflects the difficulty in modelling such a fire source in a confined and mechanically ventilated atmosphere, even with a calibration of the models.

Benchmark Step 2_2 consisted of an open simulation of the specific test carried out in open atmosphere in order to bring knowledge on the specific fire source of the real fire event and to re-calibrate the fire models on the event-like fire source between Step 2 and Step 3. The low power ignition protocol over a longer time as used in this test led to a better preheating of the cables. The predicted HRR peak is captured by the models for most of the participants but deviations from the experimental values are nevertheless observed on the duration of the incubation stage of the fire, showing the difficulty of correctly predicting the preheating of the cables. The lack of data on cable thermal inertia and cable ignition temperature contributed to these deviations, as these quantities play an important role in the preheating time of cables.

Benchmark Step 3 consisted of the simulation of the heater bay fire event. The wide variety of results, with remarkable differences between the simulation results by different codes and code users as well as in comparison to the event data, is the expression of the difference between the real fire event, what had been understood from the real cable fire event and what had been tried to simulate with the knowledge and tools available so far. The presence of an overhang above the cable trays played an important role in the estimation of the fire duration. Short fire durations are obtained if the fire plume rapidly reaches the sprinkler head position. Longer fire durations are obtained if the sprinkler head is not located in the area of the fire plume, thus allowing time for the fire to fill the ceiling with smoke, until the smoke line reaches the sprinkler elevation.

In order to overcome the difficulty in obtaining reliable input data on cable fires, the authors suggest collecting additional data by an expert group including modellers upon occurrence of an event in view of future research activities on simulating real fire events.

Acknowledgements

The authors of this paper are grateful for the financial and technical support by the OECD/NEA member countries Belgium, Finland, France, Germany, Japan, Korea, Spain, the United Kingdom, and the United States of America participating in the joint OECD/NEA PRISME 2,

PRISME 3 and FIRE Projects. We would also like to thank the IRSN LEF for conducting the PRF BCM-S2 test in support to this Benchmark Exercise.

References

[1] Organization for Economic Co-operation and Development (OECD) Nuclear Energy Agency (NEA), Committee on the Safety of Nuclear Installations (CSNI), FIRE Project Report: "Collection and Analysis of Fire Events (2010-2013) - Extensions in the Database and Applications", NEA/CSNI/R(2015)14, Paris, France, August 2015, https://www.oecd-nea.org/nsd/docs/2015/csni-r2015-14.pdf.

[2] Organization for Economic Co-operation and Development (OECD) Nuclear Energy Agency (NEA), Committee on the Safety of Nuclear Installations (CSNI): Combinations of Fires and Other Events - The Fire Incidents Records Exchange Project Topical Report No. 3, NEA/CSNI/R(2016)7, Paris, France, July 2016.

[3] P. Zavaleta, L. Audouin: Cable tray fire tests in a confined and mechanically ventilated facility, Fire and Materials, Vol. 42, Issue 1, pp. 28-43, Wiley & Sons, Hoboken, NJ, USA, 2018, https://doi.org/10.1002/fam.2454.

[4] P. Zavaleta, S. Suard, L. Audouin: Cable tray fire tests with halogenated electric cables in a confined and mechanically ventilated facility, Fire and Materials, Vol. 43, Issue 5, pp. 431-609, Wiley & Sons, Hoboken, NJ, USA, 2019.

[5] Organisation for Economic Co-operation and Development (OECD) Nuclear Energy Agency (NEA), Committee on the Safety of Nuclear Installations (CSNI): OECD FIRE Database Version 2017:02, Paris, France, May 2019 (limited to FIRE member countries only).

[6] C.K. Sze: Response time index of sprinklers, International Journal on Engineering Performance-Based Fire Codes, Number 1, p.1-6, 2009.

[7] H. Pretrel, P. Zavaleta, S. Suard: Experimental study of the influence of the mechanical ventilation on the behavior of cable tray fires in a confined compartment, Special issue PRISME 3, Fire safety Journal, to be published.

[8] S. Bascou, L. Audouin, S. Suard: Common Cable Fire Benchmark Activity of the OECD Nuclear Energy Agency Projects PRISME 3 and FIRE, in: Röwekamp, M., H.-P. Berg (Eds.): Proceedings of SMiRT 25, 16th International Seminar on Fire Safety in Nuclear Power Plants and Installations, October 28-30, 2019, Ottawa, ONT, Canada, GRS-A-3963, Gesellschaft für Anlagen- und Reaktorsicherheit (GRS) gGmbH, Cologne, Germany, December 2019, https://www.grs.de/en/publication/grs-3963.

[9] American Society for Testing and Materials (ASTM): ASTM E1355-12(2018), Standard Guide for Evaluating the Predictive Capability of Deterministic Fire Models, ASTM International, West Conshohocken, PA, USA, 2018.

[10] P.S. Sumitra: Categorization of Cable Flammability. Intermediate-Scale Fire Tests of Cable Tray Installations, Interim Report NP-1881, Research Project 1165-1, Factory Mutual research Corp., Norwood, MA (1982).

[11] K. McGrattan et al.: Cable Heat Release, Ignition, and Spread in Tray Installations During Fire (CHRISTIFIRE) Phase 1: Horizontal Trays, NUREG/CR-7010, Vol. 1, prepared

for United States. Nuclear Regulatory Commission (U.S. NRC) Office of Nuclear Regulatory Research, Washington, DC, USA, July 2012, https://www.nrc.gov/docs/ML1221/ML12213A056.pdf.

[12] A.B. Morgan, J.W. Gilman: An overview of flame retardancy of polymeric materials: application, technology, and future directions, Journal of Fire and Materials 37 (2013) 259-279.

[13] K. McGrattan et al.: Cable Response to Live Fire (CAROLFIRE) Volume 3: Thermally-Induced Electrical Failure (THIEF), NUREG/CR-6931, Vol. 3, NISTIR 7472, prepared for United States Nuclear Regulatory Commission (IU.S. NRC), April 2008, https://www.nrc.gov/docs/ML0811/ML081190261.pdf.